# Sensitivity of munitions to lightning strikes; the effect of building lay-out, munition stacking, type of EED and packaging

R.H.B. Bouma[1], E.J. Kroon, S.A.L. de Koster, H.P.A. Dijkers, F.P. Weterings
The Netherlands Organization for Applied Scientific Research (TNO)
Ypenburgse Boslaan 2, NL-2496 ZA The Hague, The Netherlands

## Abstract

The effect of lightning strikes on munition storage sites is being studied extensively by the Dutch MoD, DNV, and TNO, and comprises site reviews, risk assessments, modelling of storage sites and understanding of the link with munition sensitivity. This paper focuses on one specific part of the study: the munition sensitivity to electromagnetic effects of lightning strikes. The approach is physics-based, and aims to model the electromagnetic field distribution in a magazine from a lightning strike attachment to the structure, the effect of packaging on the damping of the electromagnetic field, the electromagnetic coupling into the electro-explosive devices (EEDs) in a munition, in order to make a comparison to known EED initiation characteristics.

The response of EEDs to an electric field, assumed proportional to the lightning strike current, was studied. It was found that the ignition is governed by the No-Fire Threshold (NFT) energy rather than the NFT power. The NFT energy is specific to each EED, which requires a worst-case approach, as a munition magazine should be able to store a wide variety of munitions.

A 3-dimensional model was constructed for a storage magazine constructed with reinforced concrete, with rebar acting as natural lightning protection system (LPS). A comparison was made to a situation with an added external LPS (air-termination, masts as down-conductors, and earth termination), not being isolated from the storage magazine. A direct comparison of electric field strength is used for the assessment of flash-over probability. It was noted that the limiting electric field strength needed careful consideration. A further initiation route is the direct coupling of the electromagnetic field into an EED (i.e. without a flash-over from the wall). The EED initiation was related to its NFT energy and dimension, assuming a maximum coupling of the electromagnetic field.

Typically, a storage magazine is modelled as an empty structure. However, the high metallic content of munitions and packaging, will influence the electromagnetic field distribution inside a magazine. A specific 3-dimensional model was therefore made to study this effect. It was found that the ratio of electric field strength and magnetic field vector in the magazine does not equal the 377 Ω impedance of air in the far field approach, and therefore limits the damping of the electromagnetic field by the ammunition boxes.

## 1 Introduction

Munition storage structures are equipped with lightning protection systems to prevent accidental ignition of munition or explosives due to lightning flash strikes on or near a storage structure. In [1] an overview is given of accidents with energetic materials and ammunition storage, covering a timespan of one century. Out of 141 accidents 8 were attributed to lightning. Often these accidents were followed by fire. For one

[1] Corresponding author: richard.bouma@tno.nl

particular accident in 1910 it is stated that "*The lightning-arresting system, which had been installed for just such an event, for some reason failed*." The peak electric currents induced by lightning strikes were monitored during circa 12 months at various storage sites in the UK [2]. The observations in that study include "*UK MOD explosives facilities collect lightning strikes. .. it is likely that many of the indications are either caused by upward leader activity, current distribution via the meshes formed by interconnected earthing systems or some other phenomena*.", and "*Low flash density does not necessarily mean there will be no potentially damaging current*." An extensive study was initiated by the Dutch MoD. DNV and TNO were tasked to perform site reviews, risk assessments, modelling of storage sites and understanding of the link between an actual lightning strike and munition sensitivity. Our approach to risk assessment is presented in [3]. Various important aspects related to munition sensitivity are covered here.

## 2 Lightning strike and munition initiation routes

When a lightning strike hits a munition storage structure, a current distributes over the rebar in the reinforced concrete and/or the external LPS. This results in a potential gradient across the conductors and an electromagnetic field (EM-field) distribution in the inner volume of the structure where energetic materials and ammunition is stored in stacks. The potential gradients and EM-field distribution depend on lightning strike wave form, location of strike attachment on the structure, and the storage structure lay-out.

Three lightning strike routes are considered:

1. Flashover to the ammunition stack may occur through dielectric breakdown of the air between the inner wall of the magazine and the stack;
2. Coupling of electromagnetic energy to the munition packaging and casing due to current distribution created in metallic components (rebar) of the magazine;
3. Coupling into EEDs of an EM-field that radiates from current flowing in the magazine.

All three initiation routes are dependent upon the lightning strike characteristics and the construction details of the munition storage structure (rebar, lightning protection masts, metal doors, *etc*.).

### 2.1 Lightning strike characteristics

Lightning strike currents cannot be described with uniform waveform parameters, see e.g. [4]. For analysis purposes the description of a current profile encompassing 99% of lightning strikes with a 200 kA peak current [5] was used, as well as the current profiles mentioned in [6, Appendix B], for the first positive 10/350 μs impulse (i.e. 10 μs rise time and 350 μs voltage surge duration), the first negative 1/200 μs impulse and the consecutive negative 0.25/100 μs impulses, with respective peak currents of 200, 100 and 50 kA.

In particular [6] mentions to use a 10% probability of the first positive impulse and 90% probability of the first negative impulse. Thereby it should be noted that each pulse shape has is its own probability density function of pulse amplitude.

The cumulative distribution function (CDF) of lightning versus peak current [6] is presented as red dots in Figure 1. It was verified whether the same CDF could be derived from the first positive and first negative impulse, see yellow curve in the figure, as the same calculation procedures will be needed in the assessment of EED ignition to lightning strike. There is a similarity for lightning currents of 20 kA and above.

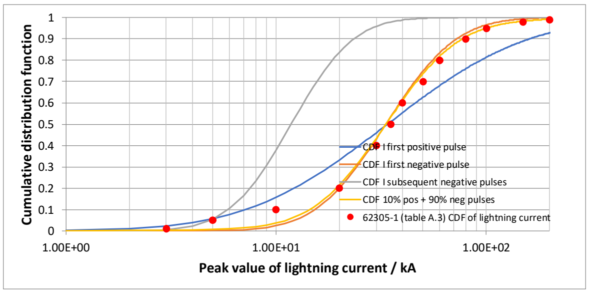


Figure 1 Cumulative distribution function of the peak value of lightning current.

### 2.2 Construction of munition storage

3-Dimensional representations were made of munition storage sites. Each digital copy of a storage structure was validated by a site review, ground resistance measurement and comparison of experimental and numerical EM-fields in response to well-known electric and electromagnetic signals. One such 3D representation is shown in Figure 2.

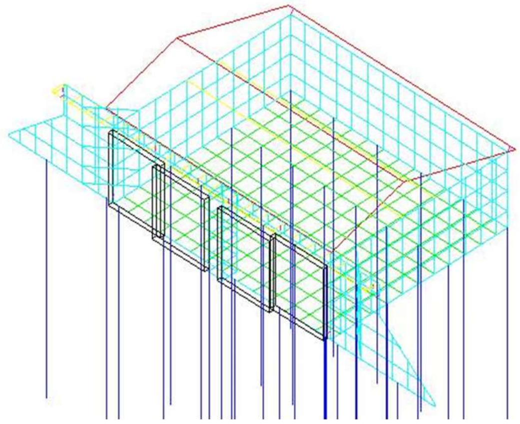

Figure 2 Representation of munition storage for lightning strike assessment [by courtesy of DNV GL].

### 2.3 EM-field distribution inside munition storage

An example of calculated EM-fields is shown in Figure 3 where lightning strikes at one of the lightning protection masts of a munition storage structure equipped with both rebar and masts as current down conductors. In this case the 100 kA negative impulse lightning strike is simulated. The electric field $E$ and magnetic field vector $H$ (which is proportional to the magnetic flux density) were evaluated at grid points located at 10 cm distance from the wall. First those grid points were identified where the electric field and the magnetic field vector reach their maximum value. The $E$ and $H$ profiles at these grid points were then used for the assessment of EED ignition.

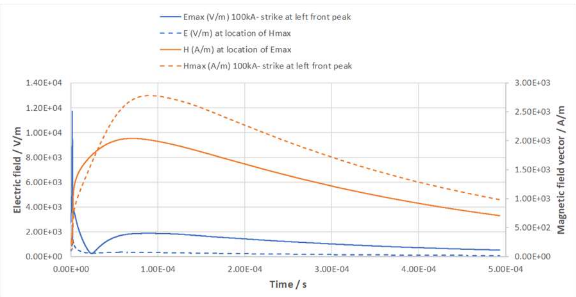


Figure 3 Electric field E (blue) and magnetic field vector H (orange) as a function of time at 10 cm distance from the wall in a storage magazine with rebar and lightning protection masts.

## 3 Ignition of EEDs

The likelihood of ignition of munitions with EEDs by an EM-field in a storage structure is determined by 1) the EM-field characteristics inside the structure, 2) the EED characteristics and 3) attenuation of the packaging material or the munition.

### 3.1 EED characteristics

EEDs in ammunition storage comprise the low voltage bridge-wire and film bridge EEDs, conducting composition EEDs, and semi-conducting initiator or semi-conducting bridge EEDs and the high voltage exploding bridge-wire EED and exploding foil initiator. Storage structures receive a wide variety of munitions and therefore all types of EEDs were considered. For the assessment of initiation the electrical energy and/or power required to initiate an EED needs to be known. The No-Fire Threshold Energy ($E_{NFT}$), the No-Fire Threshold Power ($P_{NFT}$) and the resistance $R$ [7,8] are the relevant EED characteristics when being conservative regarding the possibility of initiation. $E_{NFT}$, $P_{NFT}$, their ratio i.e. the thermal time constant $\tau$, and $R$ were required for items in the Dutch munition inventory. In particular a data set from [9,10] was used, covering a wide variety of EEDs. The $E_{NFT}$ governs the response of an EED to a short duration pulse and $P_{NFT}$ to a long duration pulse. The gradual transition of the No-Fire Threshold between both regimes near the thermal time constant is described by:

$$E_{NFT}(t_1) = \frac{P_{NFT}\, t_1}{1 - exp\left(\frac{-t_1}{\tau}\right)}$$

in case of a block wave pulse of duration $t_1$ that is typically applied in EED characterization tests.

### 3.2 Ohmic heating of EED

A model was derived that accounts for Ohmic heating of the resistive element of an EED, and heat loss from this element to the surroundings ($T$ is temperature, $t$ is time, $I(t)$ is current):

$$\frac{dT}{dt} \approx \frac{I^2(t)R}{E_{NFT}} \Delta T_{NFT} - \frac{P_{NFT}}{E_{NFT}} T$$

The model was applied to more than 170 different EEDs. As an example the results for two EEDs are shown in Figure 4, with the temperature rise to the No-Fire Threshold, $\Delta T_{NFT}$, set at a value of 300 °C. The applied current profile was assumed to be proportional to the lightning current according to Merewether [5], and its amplitude was adapted such that the maximum temperature in the EED just reaches $\Delta T_{NFT}$. The choice for a specific value $\Delta T_{NFT}$ was checked but did not influence the required current at the No-Fire Threshold, and therefore confirms that the initiation of an EED caused by a current pulse, is dominated by $E_{NFT}$ and not by $P_{NFT}$. This even holds for conduction composition EEDs which have a thermal time constant $\tau$ less than the time to reach the No-Fire Threshold temperature. In contrast to a block pulse used in characterization of EEDs, most of the energy is deposited in the EED during the initial phase of a lightning strike.

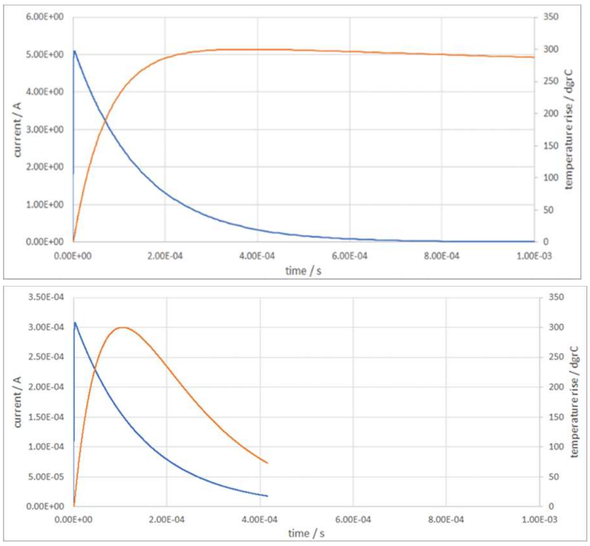


Figure 4 Current (in blue) and temperature (in orange) versus time at the No-Fire Thresholds of 1) fuzehead N38 from Davey Bickford with $R_{average}$ = 0.9 Ω, $P_{NFT}$ =133.2 mW, $E_{NFT}$ =1.71 mJ and $\tau$=12.8 ms (top) and 2) conducting composition cap M52A-3B1 with $R_{average}$ = 600 kΩ, $P_{NFT}$ =14 mW, $E_{NFT}$ = 0.0022 mJ and $\tau$=0.157 ms (bottom).

### 3.3 EM-field coupling into EED

A worst-case approach was used, to avoid underestimation of the induced current in an EED due to the presence of an EM-field upon a lightning strike on the storage structure. A maximum coupling of the electromagnetic field into the EED with associated circuitry was assumed. Two typical configurations were considered: 1) the EED is not part of a closed loop and has two open-ends, and 2) the EED is part of a closed loop. In the first case the open-ended EED acts as a dipole antenna characterized by its resistance $R_{EED}$ and dipole length $L_{ANT}$, and is sensitive to the electric field *E(t)*, see Figure 5. If $L_{ANT}$ is much smaller than the wavelength of the EM-field, and if the dipole is aligned parallel to the electric field, one can derive the induced current *I*.

$$I(t) \gtrsim \frac{E(t)L_{ANT}}{R_{EED}}$$

The likelihood of ignition of an EED exposed to the electric field component of the EM-field was assessed assuming a short duration of the field in comparison to the thermal time constant of the EED and using the No-Fire energy threshold, the EED resistance and length of the antenna, i.e.

$$\text{if } \int_0^\infty E^2(t)dt < \frac{E_{NFT}R_{EE}}{L_{ANT}^2}$$

then ignition is unlikely,
else ignition is probable or certain.


Figure 5 Schematic representation of an EED in dipole antenna configuration, and aligned parallel to the electric field vector.

In the second case the EED and circuitry acts as a loop antenna characterized by its resistance $R_{EED}$ and loop area *A*, and is sensitive to the magnetic flux density *B(t),* see Figure 6. If the square root of *A* is much smaller than the wavelength of the EM-field, and if the plane of the loop antenna is a aligned normal to the magnetic field, one can derive the voltage $V_{OC}$ across the EED.

$$V_{OC}(t) = -A\frac{dB(t)}{dt}$$

The likelihood of ignition of an EED exposed to the magnetic field component of the EM-field was assessed assuming a short duration of the field in comparison to the thermal time constant of the EED and using the No-Fire energy threshold, the EED resistance and area of the antenna, i.e.

$$\text{if } \int_0^\infty \left(\frac{dB(t)}{dt}\right)^2 dt < \frac{E_{NFT}R_{EED}}{A^2}$$

then ignition is unlikely,
else ignition is probable or certain.

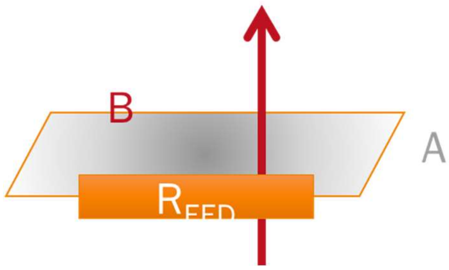


Figure 6 Schematic representation of EED in loop antenna configuration, with the normal of the loop aligned with the magnetic flux density.

The assessment of EED ignition in a dipole or loop antenna configuration, was performed using the extreme values of the product of $E_{NFT}$ and $R_{EED}$ of $5 \cdot 10^{-6}$ J$\Omega$ and $10^{1}$ J$\Omega$, as well as a characteristic length or diameter of the antenna of 0.1 m.

## 4 Assessment of flash-over and ignition of EEDs

The assessment of a flash-over from the wall to the munition stack was made by simulation of a 200 kA positive lightning impulse as well as a 100 kA negative lightning impulse, finding the location maximum electric field strength in both simulations at a 10 cm distance from the wall, the application of the respective probability density functions for lightning peak current, and finally the calculation of the electric field CDF using 10% positive and 90% negative pulses. In the example of the CDF shown in Figure 7, electric fields are always below the dielectric strength of air[2] and therefore it was concluded that no flash-over from the wall to the munition stack would occur.

The CDF of the property related to the coupling of the electric field into an EED, $\int_0^\infty E^2(t)dt$, was determined in a similar fashion. In the example of Figure 8 the criterion for the most sensitive EED is to the left of the CDF and ignition of such EED was expected. The criterion of the least sensitive EED crosses the CDF and therefore ignition of such an EED is probable depending on lightning strength.

The CDF of the property related to the magnetic field coupling, $\int_0^\infty \left(\frac{dB(t)}{dt}\right)^2 dt$, was determined for the same storage structure, see Figure 9. Again the most sensitive EED was expected to ignite. However, the least sensitive EED was expected not to ignite at all.

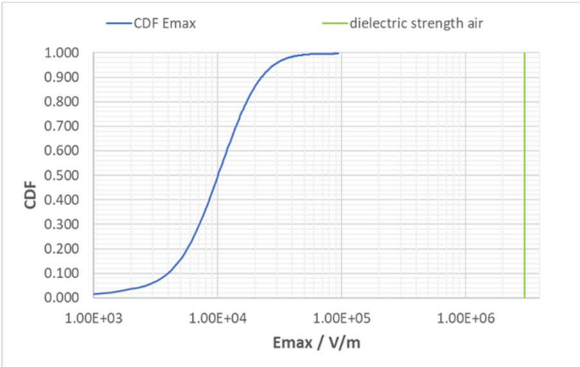


Figure 7 Cumulative distribution function of peak electric field (blue) and a flash-over criterion (green vertical bar).

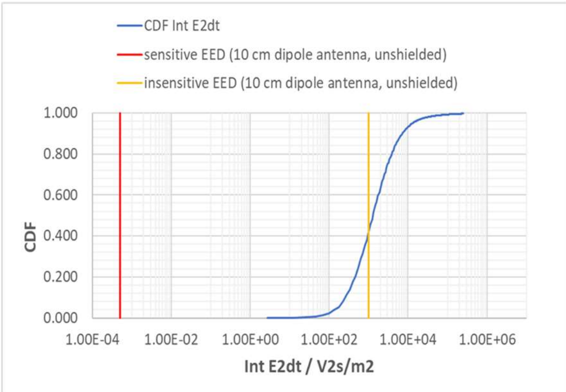


Figure 8 Cumulative distribution function of the parameter representative for the electric field coupling into an EED (blue), the criterion related to the most sensitive EED (left vertical bar) and least sensitive EED (right vertical bar).

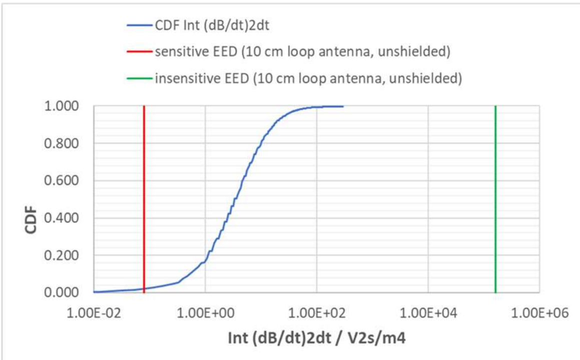


Figure 9 Cumulative distribution function of the parameter representative for the magnetic field coupling into an EED (blue), the criterion related to the most sensitive EED (left vertical bar) and least sensitive EED (right vertical bar).

Note that worst case assumptions (perfect alignment of electric field and EED, no shielding of the EED and a

[2] Note that the criterion for flash-over is less than the shown value of 3 MV/m. The actual criterion is beyond the scope of this paper.

10 cm dipole antenna) apply to the above assessments. In case of smaller EED electric circuits, ignition criteria shown as vertical bars in Figure 8 and Figure 9 will shift to the right. In case of shielding of EEDs the EM-field is reduced and the CDFs in these figures will shift to the left.

## 5 Shielding of EM-fields by munition and/or packaging

Metallic packaging as well as metallic munition casings and shells will attenuate the EM-field. The attenuation is calculated using a slightly adopted approach from Ott [11]. Firstly the metal munition box is treated as a perfect metallic envelope surrounding the munition with three contributions to the total and frequency dependent shielding effectiveness $SE_{metallic\ envelope}$ stemming from 1) absorption loss by the shield material, 2) reflection loss at the shield-air interfaces, and 3) a correction factor to the absorption loss accounting for reflections in a shield of finite thickness.
Secondly the effect of an opening between container and lid on shielding effectiveness $SE_{slot}$ is treated as attenuation decreases.
Figure 10 shows the attenuation in case of a steel ammunition box with an opening of 50 cm as a function of frequency. The frequency range covers the frequency content of lightning strikes. The left-hand side of the figure is dominated by the damping of the EM-field by a 1 mm thick steel shield while the right-hand side is dominated by EM-fields leaking through the 50 cm opening of the container. The damping of the EM-field is a function of the EM impedance of air. For a plane wave in free space the impedance is 120 $\pi$ or 377 $\Omega$. During a lightning strike the EM wave impedance, i.e. the ratio of electric field $E$ and magnetic field vector $H$, is not equal to 377 $\Omega$, see e.g. Figure 11.
In order to calculate the shielding, the EM wave impedance profile was determined at the locations of maximum $E$ and maximum $H$ at 10 cm from the wall in the storage structure. The minimum value of the EM wave impedance was determined and applied to the calculation of $SE_{metallic\ envelope}$ in the complete frequency range up to 1 MHz. The minimum of the calculated frequency dependent attenuation (both $SE_{metallic\ envelope}$ and $SE_{slot}$), like shown in Figure 10, is taken as the effective single value for attenuation by the munition packaging.

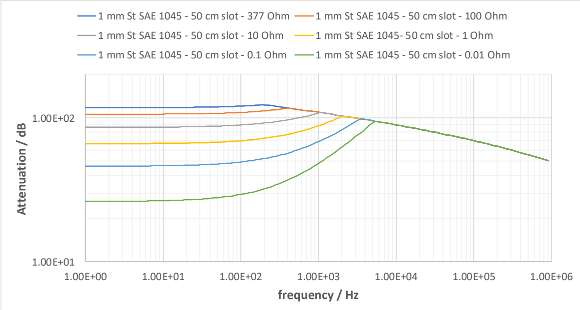


Figure 10 Double logarithmic plot of attenuation of the EM-field versus frequency, for a 1 mm thick steel ammunition box with a 50 cm opening between container and lid, for indicated EM wave impedances in air.

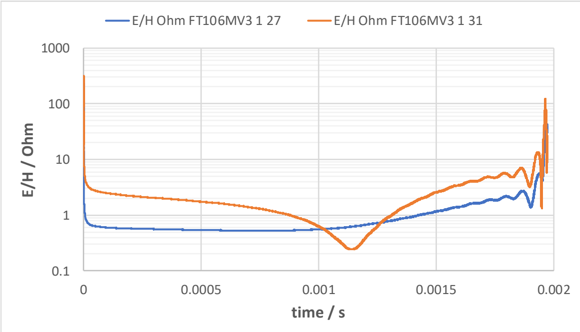


Figure 11 EM field impedance at two different locations at 10 cm from the wall in a specific magazine versus time as a result of a 100 kA negative strike.

## 6 Effect of munition stacks

The EM-field in the analysis above, was determined for the lightning strike at an empty storage site. The presence of metallic objects within the storage volume will change the EM-fields and thus may have an effect on the ignition of munitions and energetic materials. The change in EM-field depends on the location; near the wall or in the center of the storage, and the filling degree of the storage volume. A dedicated simulation was performed, see Figure 12, of a structure without and with two stacks of ammunition boxes. One stack was positioned near the wall, and one stack near the center (only half the storage structure was simulated because of symmetry). The electric field shown in Figure 12 is at one height. Both figures have the same axis for direct comparison of the electric field strengths. The position of the rebar in the wall as well as munition stack is clearly visible in these two figures. The electric field strength in the empty magazine is largest near the wall. The electric field strength increases near the wall due to the presence of the ammunition box. Inside the box, the electric field is decreased.

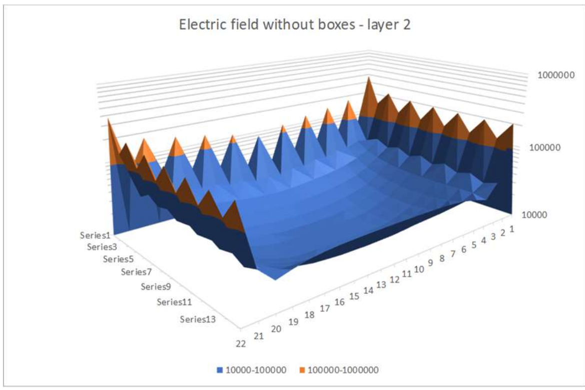


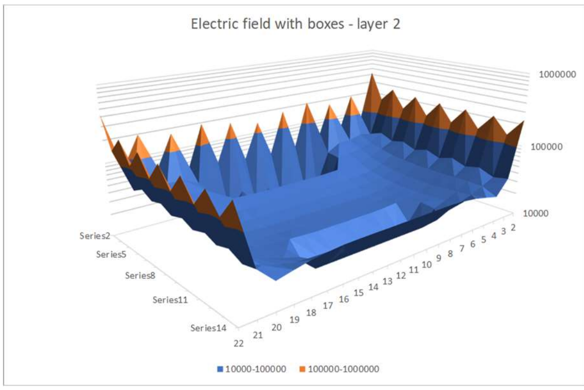


Figure 12 Simulation of electric field at one height in a storage structure without (left) and with (right) ammunition boxes near the wall and near the center.

## 7 Conclusion

A physics-based approach was developed to assess the sensitivity of munitions and energetic materials to the effects of a lightning strike on a munition storage site. The cumulative distribution function of the electric field *E* is used to assess the probability of a flash-over from the wall to the munition stack. The cumulative distribution functions of the parameters $\int_0^\infty E^2(t)dt$ and $\int_0^\infty \left(\frac{dB(t)}{dt}\right)^2 dt$ are used to assess the probability of electric and magnetic field coupling into an EED, respectively. The effect of munition boxes and munition casings on the attenuation of the electromagnetic field is included into the approach. One can identify the performance of a specific storage site regarding protection against the effect of lightning and/or identify the munition articles at risk.

## Acknowledgements

The authors gratefully acknowledge the financial support from the Dutch Ministry of Defence (Contract No. 4501381146, 8500001716 and 8500004083).

The authors also like to acknowledge the contributions from DNV, in the joint research projects for the Dutch MoD. Their contributions have provided valuable insights and enabled detailed understanding of the topic.

## References

[1] T.L. Boggs, K.P. Ford, J. Covino, Realistic safe-separation distance determination for mass fire hazards, NAWCWD TM 8668, 2013.

[2] G.R. Trout, UK lightning strike current measurements on the UK MoD explosives estate 1999-2001, 30th Explosives Safety Seminar, Atlanta, 13-15 August 2002.

[3] H.P.A. Dijkers, J.W. van Middelaar, D.G.M. van der Pol, R.H.B. Bouma, F.P. Weterings, Lightning protection on a munition storage compound – Method for safety risk assessment, PARARI 2022 Australian Explosive Ordnance Safety Symposium, Canberra, 8-10 November 2022.

[4] S. Fang, L. Zhang, L. Zou, Y. Chen, Y. Wang, Study on lightning overvoltage and commutation failure in UHV AC/DC hybrid system, J. Eng., 2019, Vol. 2019 Iss. 16, pp. 2677-2682.

[5] K.W. Merewether, Maximum lightning induced voltages and recommended isolation distances in nuclear explosive areas at Pantex, Sandia National Laboratories technical memorandum, December 13, 1997.

[6] Protection against lightning – Part 1: General principles, IEC 62305-1:2011.

[7] Electro-explosive devices, assessment and test methods for characterization – AOP-43, STANAG 4560, ed. 3, 2016.

[8] Electro-explosive devices, assessment and test methods for characterization guidelines for STANAG 4560, AOP-43, ed. 3, 2016., Issue 1, 2012.

[9] Principles for the design and assessment of electrical circuits incorporating explosive components, OB Proc 101, Issue 2, 1997.

[10] Safety principles for electrical circuits in systems incorporating explosive components, part 2, electro-explosive devices and their characterization, DEF-STAN 59-114, Issue 1, 2012.

[11] H.W. Ott, Noise reduction techniques in electronic systems, John Wiley & Sons, 1988.